ACS OMEGA

Open Access

http://pubs.acs.org/journal/acsodf

Article

Highly Electrically Conductive PEDOT:PSS Films via Layer-By-Layer Electrostatic Self-Assembly

Muhammad Khurram, Sven Neuber, Annekatrin Sill, and Christiane A. Helm*

Cite This: *ACS Omega* 2024, 9, 48810−48820

Read Online

ACCESS | Metrics & More | Article Recommendations | Supporting Information

ABSTRACT: Electrically conductive films of poly(3,4-ethylenedioxythiophene):poly(styrenesulfonic acid) (PEDOT:PSS) are usually formed by spin coating of aqueous dispersions with PEDOT:PSS nanoparticles. To better understand the film formation, the adsorption conditions are investigated using dip coating and a flow cell with different flow rates. Multilayer films are formed by sequential adsorption of oppositely charged macromolecules or nanoparticles. PEDOT:PSS serves as polyanion, and PDADMA is the polycation. In the dip coating process, the first layer consists of a ≈70 nm thick PEDOT:PSS nanoparticle monolayer. Subsequent PDADMA/PEDOT:PSS bilayers have a constant thickness (9.5 nm). Using the flow cell (0.2 mL/min) for film preparation led to constant PDADMA/PEDOT:PSS bilayer thickness (7.5 nm). PEDOT:PSS nanoparticle monolayers were only observed after PEDOT:PSS adsorption when the washing step was omitted. The electrical conductivity is independent of the number of deposition cycles for both preparation methods. Films prepared by dip coating show low conductivity (26 kS/m) and high surface roughness, whereas films prepared by flow cell show high conductivity (230 kS/m) and low roughness (2−4 nm). We propose that the adsorption in a flow cell leads to a flat orientation of the PEDOT molecules, which increases charge carrier mobility. It is hoped that a better understanding of the relationship between adsorption conditions and carrier mobility will further improve electrical conductivity.

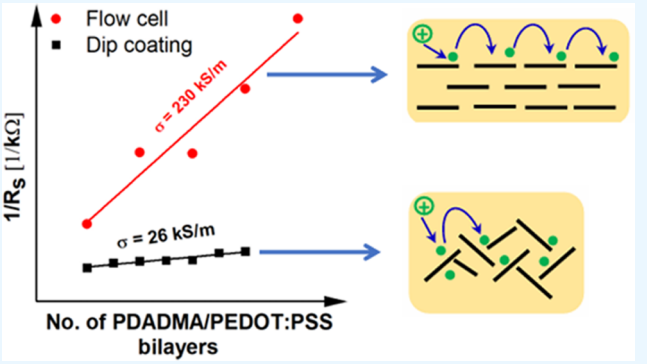

1. INTRODUCTION

We aim to prepare thin organic films with high electrical conductivity and tunable sheet resistance for biomedical applications. For the conducting polymer, we chose PEDOT:PSS (poly(3,4-ethylenedioxy-thiophene):poly-(styrenesulfonate)). Spin-coated PEDOT:PSS films have a DC conductivity of close to 10^5 S/m (1000 S/cm), making them the material of choice for organic electrical devices.[1−3] However, PEDOT:PSS films are unstable in aqueous solutions.[4−7] Films prepared by mixing PEDOT:PSS with another emulsion were stable.[4] However, these films had a lower conductivity than spin-coated PEDOT:PSS films (2.9×10^4 S/m).

Stability in water may be achieved if the films are made from a polymer mixture. Therefore, films were built using a layer-by-layer technique (LbL) by sequentially adsorbing oppositely charged polyelectrolytes onto a substrate.[8] The versatility of the LbL method lies in the wide variety of compounds that can be deposited: polyelectrolytes, proteins, polysaccharides, clays, and inorganic nanoparticles.[9] The number of polycation/polyanion bilayers deposited controls the film thickness within a few nm.[8,10,11] This is useful because the sheet resistance depends on the film thickness ($R_S \propto 1/d$ where R_S is the sheet resistance and d is the film thickness), and R_S must be adjusted for biomedical applications.

The interest in electrochemical devices covered by thin, mechanically stable solid films led to the study of LbL films consisting of polymers only. The first study of the impedance and dielectric characteristics used films constructed from two representative polycation/polyanion pairs: PSS and PAH (poly(allylamine hydrochloride)) or PAA (poly(acrylic acid)) and PAH.[12] Electrical conductivities in the range of 10^{-10} to 10^{-5} S/m have been observed.[13−16] To increase the electrical conductivity, layers of charged electrically conductive nanoparticles (NP) or conducting polyelectrolytes replaced some polyanion layers. Films made from gold NPs showed a low electrical conductivity (≈2 S/m) since polymer molecules separated the gold NPs.[17] Another approach is the use of MXenes. Conductivities between 10^3 and 5×10^4 S/m have been reported, depending on the selected MXene and the number of deposited MXene/polycation bilayers.[18] In some cases, the DC conductivity was dependent on the number of

Received: September 30, 2024
Accepted: November 5, 2024
Published: November 25, 2024

Scheme 1. Cross Section of PEDOT:PSS Nanoparticle[a]

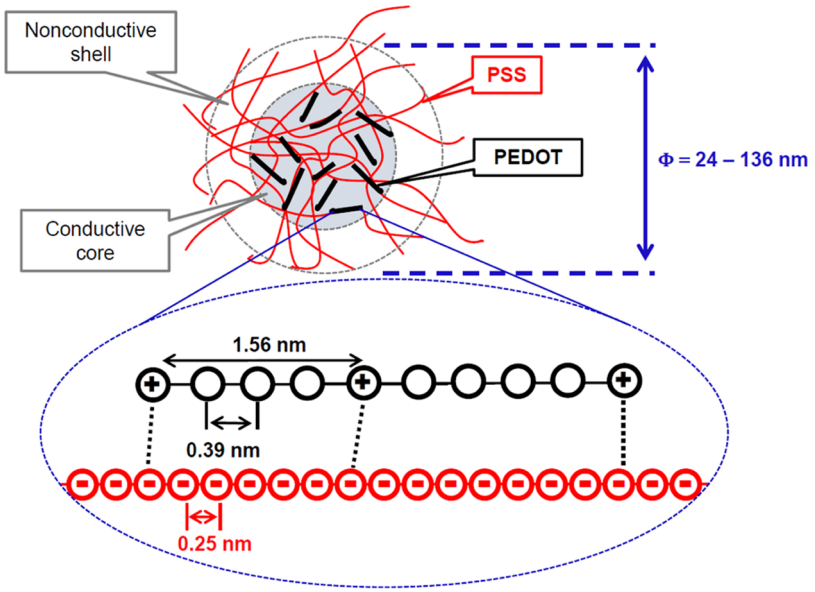

[a]The diameter (24−136 nm) is derived from X-ray diffraction studies of spin-coated films.[25] PEDOT and PSS are sketched below to illustrate the molecular dimensions involved. PEDOT consists of 10−20 repeat units; a 3rd to a 5th are charged.[30] PSS consists of several hundred to more than a thousand charged repeat units.

MXene/polycation bilayers deposited.[18] It is desirable that the electrical conductivity is independent of the number of NP/polycation bilayers deposited.

PEDOT:PSS dissolved in water is a dispersion of PEDOT:PSS nanoparticles. PEDOT is a positively charged ionomer that is insoluble in water. But it forms stable nanoparticles in water when paired with the negatively charged polyelectrolyte PSS.[19−22] These nanoparticles show a micelle-like arrangement with a hydrophobic PEDOT core and a hydrophilic PSS shell (cf. Scheme 1).[22−24] According to X-ray measurements of spin-coated films,[25] the diameter of the nanoparticles is 24−136 nm (Scheme 1). The radius is measured in the surface plane and may exceed the value found in solutions since spin-coating flattens the nanoparticles.[26] To increase the conductivity, ethylene glycol (EG) is added to the PEDOT:PSS solution. The effect is related to optimized molecular $\pi-\pi$-stacking distances (interchain coupling).[27,28]

Charged PEDOT is electrically conductive due to a polaron or bipolaron state, but PSS is not electrically conductive. High DC conductivity is only achieved when charge carriers find a percolative path.[25,29] "Percolative paths are those where charges can jump along the same PEDOT chain or between the neighboring $\pi-\pi$ stacked chains."[30] In this context, it is important to consider the orientation of the PEDOT molecules relative to the substrate surface. The roughness of spin-coated PEDOT:PSS films is low (1.2−1.7 nm).[3,26] The persistence length (3−4.5 nm) of PEDOT:PSS in solution doped with high amounts of EG[31] exceeds the surface roughness (1.2−1.7 nm) by a factor of 2. Thus, the film roughness is lower than the persistence length of the PEDOT molecules. These numbers suggest that the PEDOT molecules in the spin-coated films with high DC conductivity are oriented parallel to the substrate surrface.

A LbL film consists of many adsorbed PEDOT:PSS and polycation layers. As polycation poly(diallyldimethyl-ammonium chloride) (PDADMA) was used. Both PDADMA and PSS are strong polyelectrolytes; each repeat unit is charged. In contrast, PEDOT is a weak polyelectrolyte; every third to every fifth repeat unit is charged.[30] Due to the large distance between charges in the PEDOT molecule, every fifth to eighth PSS monomer unit binds electrostatically to a PEDOT monomer (length per monomer: 0.25 nm for PSS and 0.39 nm for PEDOT).[32,33] Depending on the synthesis method, a PEDOT molecule consists of 10−20 repeat units[30] (cf. Scheme 1). Thus, when PEDOT:PSS is adsorbed, long PSS chains with many weakly electrostatically bound PEDOT molecules adsorb.

Due to the weak electrostatic binding of PEDOT to PSS, one imagines that the adsorption conditions influence the PEDOT coverage and the orientation of PEDOT molecules within the films and, thus, the DC conductivity. We have used two methods to form thin films: (i) dip-coating: after each adsorption step, the film is removed from the solution and washed or dried, depending on the top layer[8] (ii) flow cell: the film is exposed to the continuous flow (0.2 mL/min) of adsorption or washing solutions, respectively[34] (Scheme 2). To better understand the adsorption in the flow cell (PDADMA/PEDOT:PSS)$_2$ films were prepared at different flow rates. The film thickness was monitored with ellipsometry. UV/vis−IR spectroscopy observed the absorbance spectra of polarons or bipolarons in PEDOT,[35,36] thus changes in PEDOT coverage were monitored. With AFM, film/air roughness was determined. Electrical properties, including current−voltage plots of DC electrical conductivity, were determined in dependence on the number of PDADMA/PEDOT:PSS bilayers.

A higher PEDOT:polymer ratio does not necessarily lead to higher electrical conductivity. We suggest that the adsorption conditions can influence the coverage and the nanoenvironment of the PEDOT molecules. This, in turn, influences the DC conductivity.

https://doi.org/10.1021/acsomega.4c08946
ACS Omega 2024, 9, 48810−48820

Scheme 2. Two Methods Used to Produce Multilayer Films Are Dip Coating and the Flow Cell[a]

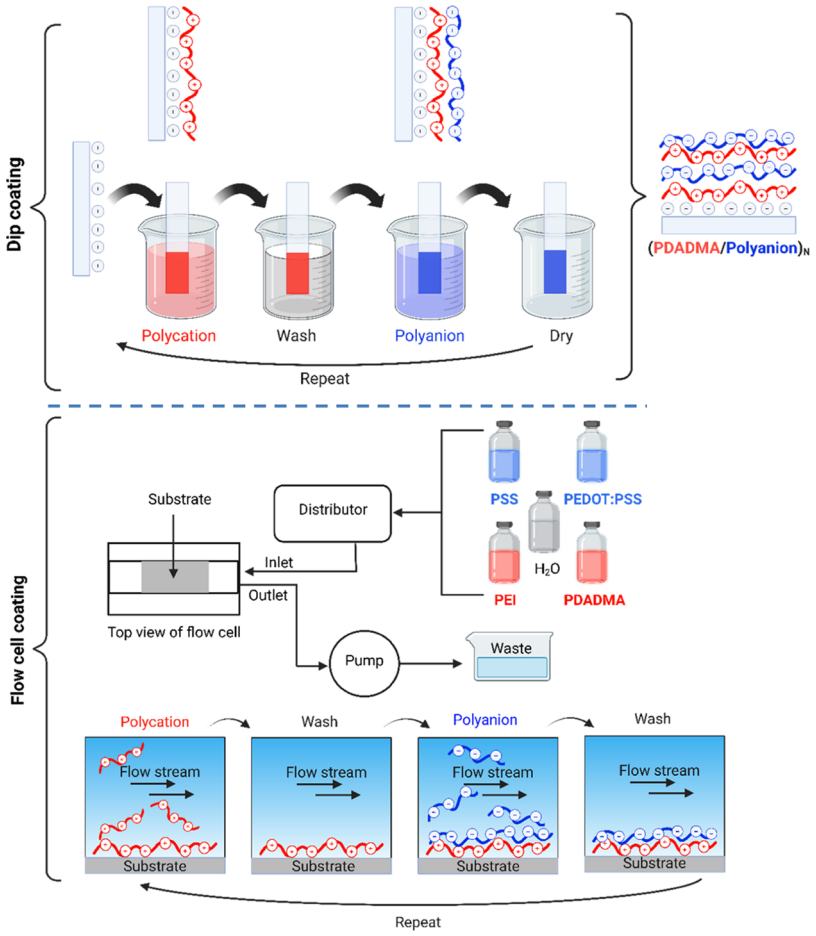

[a]The multilayer built-up is based on sequential adsorption of oppositely charged polyelectrolytes. In dip coating, the substrate is immersed in a polyelectrolyte solution and washed. After each deposition or washing step, the film is exposed to air. In the flow cell, each solution flows continuously over the substrate. The substrate is always wet. After successful film preparation, the films are removed from solution and exposed to air.

2. MATERIALS AND METHODS

2.1. Materials. The conducting polyanion PEDOT:PSS (poly(3,4-ethylenedioxythiophene) polystyrenesulfonate, Clevios PH 1000; 1.3 wt % in the aqueous dispersion) was obtained from Heraeus Deutschland GmbH & Co. KG (Hanau, Germany). The ratio between PSS and PEDOT repeat units is 1:2.5.[37] 250 mL of the industrial solution was mixed with 5 v/v % ethylene glycol (EG) (Sigma−Aldrich Chemie GmbH, Steinheim, Germany) and stirred for 2.5 h at ambient conditions.[38,39] Additionally, 3-glycidyloxypropyltrimethoxysilane (GOPS, 0.25 v/v %, Sigma−Aldrich) was added to the prepared mixture, which has been proven to prevent dissolution and delamination of PEDOT:PSS films.[5,40,41] To ensure a uniform distribution of GOPS, the solution was sonicated for 15 min. The PEDOT:PSS solution was diluted with ultrapure water by a factor of 2. The polyanion poly(ethylenimine) (PEI; M_w = 750 kDa, PDI = 12.5) was purchased from Sigma−Aldrich, the polycations poly(diallyldimethylammonium) chloride (PDADMA; M_w = 23.6 kDa, PDI = 1.88), and poly(styrenesulfonate) sodium salt (PSS; M_w = 679 kDa, PDI ≤ 1.2) were purchased from Polymer Standards Service (Mainz, Germany). For the polyelectrolyte solutions, the composition of the adsorption solution was 1 mM polyelectrolyte, with respect to the monomer concentration, and 100 mM NaCl (Merck KGaA, Darmstadt, Germany). All solutions were prepared with ultrapure water using a reverse osmosis system (Sartorius arium advance, Göttingen, Germany) followed by a Sartorius Arium Pro purification system (nominal conductivity, 0.054 μS/cm).

Microscope slides (76 mm × 26 mm, Carl Roth GmbH + Co. KG, Karlsruhe, Germany) and single-side polished silicon wafers (Silicon Materials, Kaufering, Germany) served as substrates. Quartz glass slides were obtained from Micro to Nano BV, Haarlem, The Netherlands. Before the sample preparation, the microscope glass slides and silicon wafers were cleaned according to the RCA-1 cleaning method.[42] The substrates were immersed into a solution with a 1:1:5 ratio of 32% ammonia solution (Carl Roth GmbH + Co. KG, Karlsruhe, Germany), 30% hydrogen peroxide (Carl Roth), and ultrapure water respectively, and heated to 75 °C. Afterward, the substrates were washed thoroughly with ultrapure water.

2.2. Film Preparation. The multilayer (layer-by-layer) films were prepared with two methods: dip coating and flow cell (Scheme 2).[34,43] For each method, the initial polycation/polyanion bilayer was PEI/PSS, subsequently *N* PDADMA/PEDOT:PSS bilayers were deposited.

https://doi.org/10.1021/acsomega.4c08946
ACS Omega 2024, 9, 48810−48820

Scheme 3. Side View (Left) and Top View (Right) of an Electrically Conductive Film on a Non-conductive Glass Substrate[a]

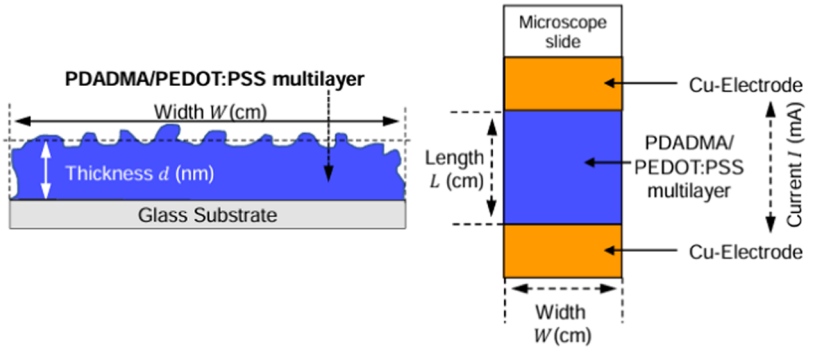

[a]The sheet resistance of the thin film depends on its dimensions: length (L), width (W), and thickness (d).

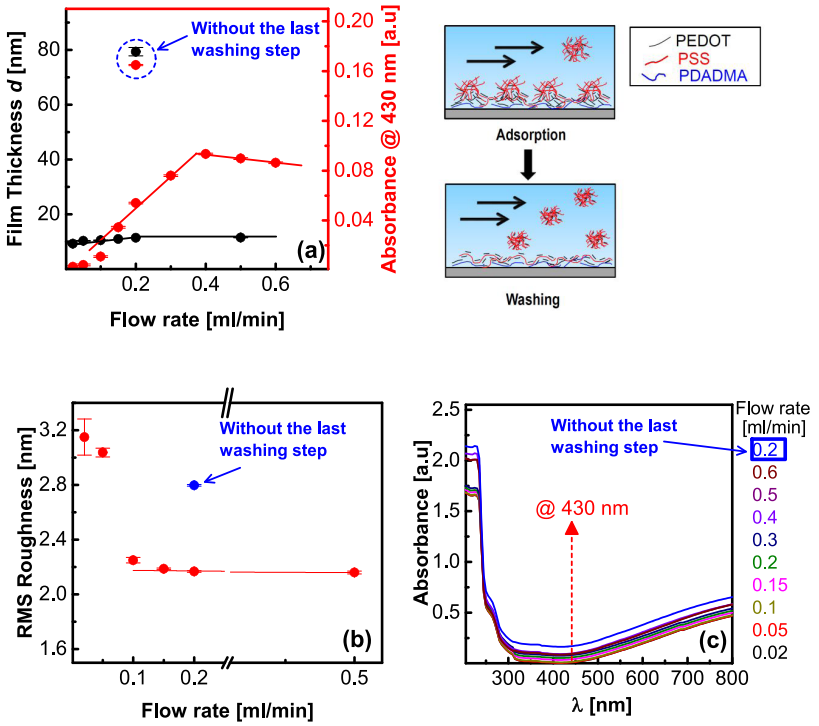

Figure 1. $(PEI/PSS)/(PDADMA/PEDOT:PSS)_2$ films prepared in the flow cell at different flow rates, in one case without the last washing step (blue). Shown are (a) the film thickness as determined with ellipsometry (index of refraction n in Table S1) and the absorbance at 430 nm, (b) the RMS roughness measured with AFM, and (c) the absorbance spectra. Also shown is a schematic of PEDOT:PSS adsorption and subsequent washing. In (a) and (b) the straight lines are linear fits. All measurements were performed in ambient air conditions. PDADMA, PSS, and PEI were adsorbed from a 0.1 M NaCl solution, and PEDOT:PSS from a salt-free solution.

Multilayers were prepared by dip coating with a computer-controlled robot (Riegler & Kirstein, Berlin, Germany)[44−49] for 15 min for each adsorption step, which we used before.[10,11] For PDADMA-terminated films, three washing steps in ultrapure water for 1 min each followed. In contrast, PEDOT:PSS terminated films were air-dried using a gentle nitrogen stream after each deposition step. All solutions are kept at 20 °C during the absorbance process using a thermostat (Thermo Scientific, Haake A25, Haake AC200). Alternatively, the multilayer was prepared in a homemade flow cell suitable for glass and silicon substrates (cf. Figure S1). A self-written LabVIEW program controls the duration of each adsorption step and the flow rate. A fluid distribution system (Rheodyne, IDEX Health and Science, Oak Harbor, WA) and a pump (ISMATEC, VWR International GmbH, Germany) are used. The PDADMA solution and PEDOT:PSS dispersion flow along the substrate at the selected flow rate. After 15 min of adsorption, 10 min of washing with ultrapure water follows.

2.3. UV/Vis−IR Spectroscopy. Absorbance measurements were performed with a UV/vis spectrometer Lambda 900 from PerkinElmer (Wiesbaden, Germany) using a wavelength range of 300−800 nm. The coated films on microscopic slides were measured directly at ambient conditions (20 °C and relative humidity 35%). To obtain the absorbance of a film prepared with dip coating, the absorbance values were divided by two because the slide was covered at both sides with identical films (cf. Scheme 1). A baseline was subtracted from the pure substrate (simple glass or quartz glass) from absorbance data. The measurements were carried out with a scan rate of 1 nm/s steps and an integration time of 1 s per step.

2.4. Null-Ellipsometry. The thickness d (in air) of PDADMA/PEDOT:PSS film was determined using null

https://doi.org/10.1021/acsomega.4c08946
ACS Omega 2024, 9, 48810−48820

ellipsometry with a He−Ne laser (power 4 mW, wavelength λ = 632.8 nm) as the light source (Multiskop, Optrel GbR, Sinzing, Germany in a PCSA [polarizer−compensator−sample−analyzer] configuration). Silicon served as substrate. The PDADMA/PEDOT:PSS film is characterized by its thickness d and complex refractive index $n - i\cdot\kappa$, where n is the real and κ the imaginary part of the refractive index. To derive the three film parameters d, n, and κ, ellipsometric angles Ψ and Δ at various angles of incidence (ranging from 66 to 72° in 1° steps) were measured.[50,51]

However, determining three film parameters based on only two independently measured values (Ψ and Δ) could introduce uncertainties due to parameter cross-coupling. To mitigate this, the light absorbance (A) was measured independently using UV/vis−NIR absorbance spectroscopy at a wavelength of 635 nm. According to the Beer−Lambert law, the absorbance A is related to the extinction coefficient $\alpha = \ln(10)\cdot A/d$, which, in turn, is connected to the imaginary part of the index of refraction: $\kappa = \alpha\cdot\lambda/(4\pi)$. Consequently, in the analysis of ellipsometric data, κ was independently determined using the condition $\kappa(A, d) = \ln(10)\cdot A\cdot\lambda/(4\pi\cdot d)$. This approach reduced the effective number of fitted parameters to two (d and n). The indices of refraction used for fitting are given in Table S1.[10,52]

2.5. Electrical Conductivity. As shown in Scheme 3, the setup involves an electrically conductive film covering a glass slide. The ohmic resistance $\left(R = \frac{U}{I}\right)$ is measured using an ELNEOS FIVE multimeter (Ernst Fischer GmbH + Co.KG, Freudenstadt, Germany) under ambient conditions (35% r.h., 20 °C). Here, R denominates the resistance, U the applied voltage, and I the current. The sheet resistance is determined according to the following

$$R_S = \frac{1}{\sigma}\frac{L}{W\cdot d} \tag{1}$$

With L the length and W the width of the film. σ denominates the electrical conductivity. The electrical resistivity ρ is the inverse of the electrical conductivity ($\sigma = 1/\rho$).[53,54]

3. RESULTS AND DISCUSSION

3.1. Adsorption Conditions. As a first step, we prepared films in the flow cell with different flow rates. We functionalized the substrate with a PEI/PSS bilayer. (We used glass, quartz glass, and silicon as substrates. For reproducibility, each substrate was functionalized similarly.) After selecting a flow rate, we used the same flow rate for all solutions and all following steps. The flow rate was varied between 0.02 and 0.5 mL/min. PEI/PSS/(PDADMA/PEDOT:PSS)$_2$ films were prepared (Figure 1).

The film thickness was determined using null-ellipsometry. The film thickness increased linearly with the flow rate up to 0.2 mL/min (from 9 to 11.5 nm), then it was constant (at 11.5 nm) (Figure 1a). We have omitted the final washing step to understand better the formation of an adsorbed PEDOT:PSS layer. The film (flow rate 0.2 mL/min) was dried immediately after PEDOT:PSS adsorption. The film thickness increased by a factor of 7 (to 79 nm, cf. Figure 1a). The sudden thickness increase suggests that PEDOT:PSS nanoparticles adsorbed and formed a monolayer with a diameter of ≈68 nm (=79.3 − 11.4 nm). This diameter is consistent with spin-coated colloids' in-plane diameter (24−150 nm).[25] Note that spin-coating flattens the particles,[29] and drying causes them to shrink vertically. The nanoparticle diameter in the solution probably exceeds 68 nm.

From the AFM images, the root-mean-square (RMS) roughness of the PEI/PSS/(PDADMA/PEDOT:PSS)$_2$ film was determined (Figure 1b). The roughness decreases with increasing flow rate up to 0.2 mL/min and remains constant (2.16 nm). The low roughness indicates that the PEDOT molecules adsorb rather flatly.

Furthermore, Figure 1c shows the UV/vis−NIR absorbance spectra between 250 and 800 nm of the films built with different flow rates. Independent of the flow rate, the absorbance spectra have a minimum at ≈430 nm, then the absorbance increases with increasing wavelength. The increasing absorbance at wavelengths exceeding 430 nm is typical for the absorbance spectra of polarons and bipolarons in PEDOT molecules.[35] Neutral PEDOT shows no absorbance in this frequency range.[36] The absorbance at 430 nm is taken as a measure of PEDOT coverage (Figure 1c). For comparison, the absorbance at 500 and 700 nm was also determined as a function of the flow rate. Qualitatively, the same increase and decrease in PEDOT coverage were observed (cf. Figure S2) for each selected wavelength.

At a flow rate of 0.02 mL/min, the absorbance of PEDOT and, thus, the PEDOT surface coverage is very low. Between 0.05 mL/min and ≈0.35 mL/min, it increases linearly, then it decreases linearly. The change of the flow rate from 0.02 mL/min to ≈0.035 mL/min causes an increase in film thickness by 20%, while the PEDOT content increases by more than an order of magnitude. At flow rates exceeding ≈0.35 mL/min, the film thickness is constant, and the coverage of PEDOT deduced from the absorbance reaches a maximum (cf. Figures 1a,c and S2). To better understand the PEDOT behavior, it is helpful to consider the PSS coverage. The absorption peak of PSS is at 225 nm.[8] However, PEDOT influences the absorption of PSS. A maximum at ≈225 nm can be observed (cf. Figure 1c), but the decline at low wavelengths is less pronounced as observed for PDADMA/PSS films.[55] Therefore, the absorbance at 225 nm is only a qualitative measure of PSS coverage. Figure S3 shows that the PSS coverage is larger at flow rates exceeding 0.35 mL/min (increased from 1.71 to ≈2.03), suggesting that these large flow rates increase the PSS coverage while they decrease the PEDOT coverage. Therefore, all of the following experiments were carried out at a flow rate of 0.2 mL/min.

To better understand the PEDOT:PSS adsorption, we measured the absorbance of the film, which was prepared without the final washing step (Figure 1a−c). The thickness measurements showed an additional PEDOT:PSS nanoparticle monolayer on top of the multilayer (≈70 nm thick). Furthermore, the nanoparticle monolayer caused a pronounced increase of the PEDOT absorbance at 430 nm of 0.11 (from 0.055 to 0.167). The PSS absorbance at 225 nm is also increased (from 1.71 to 2.41). We conclude that a PEDOT:PSS nanoparticle monolayer adsorbs when nanoparticles flow through the cell. Initially, the outer shell of the PEDOT:PSS nanoparticles consist of negatively charged PSS. However, now PSS with electrostatically bound PEDOT adsorbs onto the positively charged surface. We suggest that the nanoparticles rearrange internally allowing PSS chains with associated PEDOT molecules to move from the interior of the nanoparticle to the substrate surface and adsorb there. These PSS chains with electrostatically bound PEDOT molecules remain on the substrate surface during the washing step while

https://doi.org/10.1021/acsomega.4c08946
ACS Omega 2024, 9, 48810−48820

the altered nanoparticle monolayer consisting of PSS and PEDOT is removed.

The charge density of PSS with electrostatically bound PEDOT is effectively reduced. When a polyanion adsorbs onto a polycation-covered surface during LbL film build-up, the monovalent anions that shield the positive surface charge are replaced by polyanions. If the polyanion has a low linear charge density, then more polyanions are required than for polyanions with a high linear charge density. For this reason, the polycation/polyanion bilayers of weak polyelectrolytes are much thicker than those of strong polyelectrolytes.[56] PDADMA/PSS bilayers prepared from 100 mM NaCl solution have a thickness of ≈5 nm.[57,58] Thus, for the (PEDOT:PSS/PDADMA) bilayer, a thickness larger than 5 nm is expected.

3.2. Multilayer Thickness. Multilayers were prepared with the classical dip coating technique and by flow cell. Since a flow rate of 0.2 mL/min provides high (PDADMA/PEDOT:PSS) bilayer thickness and good coverage, we prepared films of 8 and 10 bilayers by flow cell with the same flow rate (Figure 2).

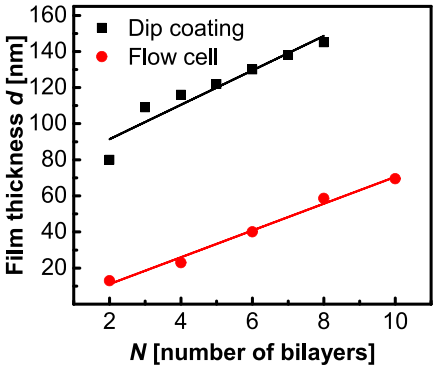

Figure 2. Thickness of PEI/PSS/(PDADMA/PEDOT:PSS)$_N$ films in dependence of N, the number of deposited PDADMA/PEDOT:PSS bilayers. Films were prepared by dip coating (black squares) and flow cell (red circles). Straight lines are linear fits. All measurements were performed in ambient air conditions using ellipsometry (indices of refraction in Table S1). PDADMA, PSS, and PEI were adsorbed from a 0.1 M NaCl solution, and PEDOT:PSS from a salt-free solution.

First, we look at the films prepared by the flow cell. Here, the film growth is linear, with a constant thickness of a PDADMA/PEDOT:PSS bilayer (7.5 ± 0.4 nm). The first two (PDADMA/PEDOT:PSS bilayers) have a somewhat lower bilayer thickness (the offset of the linear fit is −3.76 nm). Second, we look at the films prepared by dip coating. The (PEI/PSS)(PDADMA/PEDOT:PSS)$_2$ film is much thicker (80 nm) than the corresponding films prepared by the flow cell (8.5−12 nm cf. Figure 1a). The 68−71.5 nm thickness difference indicates a PEDOT:PSS nanoparticle monolayer. After the deposition of (PEI/PSS)(PDADMA/PEDOT:PSS)$_2$, the film thickness increases linearly with the number of deposited bilayers (9.5 ± 1.3 nm per (PDADMA/PEDOT:PSS) bilayer). From the second deposited PEDOT:PSS layer onward, a PEDOT:PSS adsorption layer forms, similar to the process observed in the flow cell. To stabilize the multilayer, after each PEDOT:PSS adsorption step, the film was dried with a gentle stream of nitrogen.

Note that in the linear growth regime, the average thickness of a (PDADMA/PEDOT:PSS) bilayer (9.5 nm for the dip coating and 7.5 nm for the flow cell) exceeds the thickness of a simple PDADMA/PSS bilayer (≈5 nm) adsorbed from a solution with similar ion concentrations. This observation agrees with a decreased linear charge density of PSS due to electrostatically bound PEDOT.

3.3. Surface Topography. With atomic force microscopy (AFM), the surface morphology of the PDADMA/PEDOT:PSS films was studied (Figure 3). First, we studied the films prepared by dip coating. The first PDADMA/PSS:PEDOT bilayer showed a granular structure (Figure 3, left image in the top row). Granular structures were observed before for films containing PEDOT:PSS.[35,38] On addition of further PDADMA/PEDOT:PSS bilayers, the film surface showed randomly distributed height variations attributed to aggregates. These aggregates became more abundant with an increasing number of bilayers. As a measure of the increasing height variation, the height scale of the false color representation of the AFM images is shown in Figure 3 (insert in the bottom row, increase from 67 to 111 nm). If we use the same height scale for all AFM images, then the films made of a few bilayers appear homogeneous.

Films prepared by the flow cell show a different surface morphology. The topology appears less structured (Figure 3, bottom rows) than the one of the films prepared by dip coating. The AFM images showed smaller aggregates within the surface plane. Furthermore, for the first PDADMA/PEDOT:PSS bilayer, the height variation of the aggregates was small and did not increase much with the addition of further PDADMA/PEDOT:PSS bilayers. Thus, the height scale rises slightly (from 11.5 to 32.6 nm, cf. Figure 3, insert in bottom row).

From the AFM images, the root-mean-square (RMS) roughness was determined (Figure 4). Independent of the preparation method, the roughness of PDADMA/PEDOT:PSS films increases linearly with the number of deposited bilayers. However, the roughness of films prepared with dip coating starts with a higher value and shows a steeper increase (an increase from 11.3 to 16 nm vs an increase from 2.3 to 3.6 nm). Such a low roughness, as achieved for films prepared with the flow cell, was also observed in spin-coated films with high electrical conductivity.[59,60] The low roughness indicates films with PEDOT molecules oriented approximately parallel to the surface plane.

A rough nanoparticle monolayer is the first layer of the films prepared with dip coating. The roughness increases as the number of layers increases. This indicates an arbitrary orientation of the PSS and PEDOT molecules. In the flow cell, there is a liquid flow during adsorption. Therefore, fewer molecules (note the lower bilayer thickness) adsorb in a flatter orientation.

3.4. PEDOT:PSS Surface Coverage. Figure S4 shows the UV/vis−NIR absorbance spectra between 300 and 800 nm. PDADMA/PEDOT:PSS films prepared by dip coating (Figure S4a) and flow cell (Figure S4b) were investigated. The absorbance spectra are very similar to those in Figure 1c. Each absorbance spectrum has a minimum of ≈430 nm, and the absorbance increases with an increasing number of deposited PDADMA/PEDOT:PSS bilayers. Again, the absorbance at 430 nm is taken as a measure of PEDOT coverage.

Figure 5 shows the absorbance at 430 nm as a function of the number of PDADMA/PEDOT:PSS bilayers deposited. For the films prepared in the flow cell (starting from two deposited PDADMA/PEDOT:PSS bilayers) the absorbance increases linearly with the number of deposited bilayers. The

https://doi.org/10.1021/acsomega.4c08946
ACS Omega 2024, 9, 48810−48820

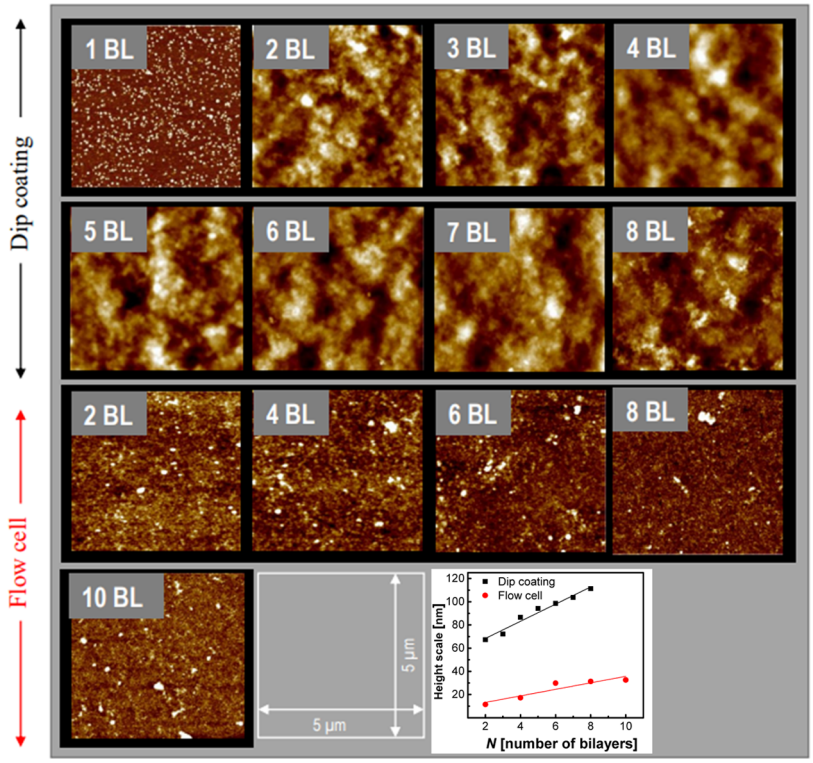

Figure 3. AFM images (5 μm × 5 μm) of the topography of PEI/PSS/(PDADMA/PEDOT:PSS)$_N$ films in dependence of the number of deposited PDADMA/PEDOT:PSS bilayers (BL). Films were prepared by dip coating (top rows) or flow cell (bottom rows). Insert (bottom right): The height scales used for the false color representation of the AFM images (from 0 nm to maximum height) versus the number of deposited bilayers. Lines are linear fits. Measurements were performed in air at r.h. = 35%.

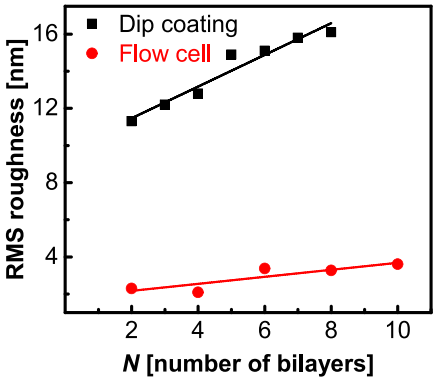

Figure 4. Roughness of PEI/PSS/(PDADMA/PEDOT:PSS)$_N$ in dependence on the number of deposited PDADMA/PEDOT:PSS bilayers. Films prepared by dip coating and flow cell are shown. The root-mean-square (RMS) roughness was calculated from the AFM images shown in Figure 3. The straight lines are linear fits.

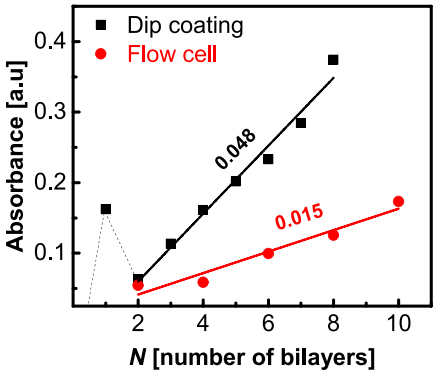

Figure 5. Absorbance at 430 nm as a function of the number of (PDADMA/PEDOT:PSS) bilayers. The thick, straight lines are linear fits, indicating the absorption increase per deposited bilayer. The dashed line shows the increase in absorbance after the adsorption of one PEDOT:PSS nanoparticle monolayer and the subsequent decrease after the adsorption of a PDADMA monolayer, which caused the removal of PEDOT.

PDADMA/PEDOT:PSS films prepared by dip coating show a maximum at one bilayer, then the absorbance drops, and from two bilayers on increases linearly with the number of deposited bilayers. The linear increase is easy to understand. The constant slope shows that the surface coverage of PEDOT is the same for each bilayer. The PDADMA/PEDOT:PSS films prepared by dip coating have a high slope (0.048 per bilayer), whereas the films prepared in a flow cell show a slope lower by a factor of 3 (0.015 per bilayer). The flow cell films, therefore, have a lower PEDOT content per deposited PEDOT:PSS/PDADMA bilayer.

The absorbance of the first (PEDOT:PSS/PDADMA) bilayer prepared by dip coating shows a maximum (0.162 at 430 nm) in the plot of absorbance versus number of bilayers. The first bilayer contains a very high amount of PEDOT. The thickness measurement (Figure 2) suggests that the first deposited PEDOT:PSS layer is a ≈70 nm thick PEDOT:PSS nanoparticle monolayer. It is expected and found that the thick PEDOT:PSS nanoparticle layer contains many PEDOT molecules. However, when the next PDADMA layer is adsorbed onto the PEDOT:PSS nanoparticle monolayer with dip coating, most PEDOT molecules are removed and

https://doi.org/10.1021/acsomega.4c08946
ACS Omega 2024, 9, 48810−48820

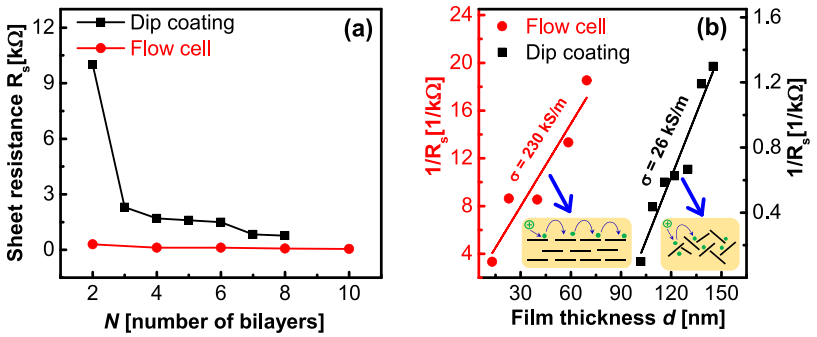

Figure 6. Electrical properties of PEI/PSS/(PDADMA/PEDOT:PSS)$_N$ films. (a) Sheet resistance R_S versus the number of deposited PDADMA/PEDOT:PSS bilayers for both preparation methods. (b) Inverse sheet resistance $1/R_S$ as a function of film thickness, note the different scales on the right and left y-axis. The straight lines are linear fits. The electrical conductivity σ is determined from the slope. The yellow schemes are a side view of the charge carrier movement for films prepared by flow cell and dip coating.

replaced by PDADMA molecules. This is an example of the building principle of polyelectrolyte multilayers.[8] Entropically, it is more favorable than a few molecules with many positive charges (such as PDADMA with M_w = 23.6 kDa corresponding to a degree of polymerization of 126, i.e., 126 positive charges along the 79 nm long chain) replace many molecules with a few positive charges (such as PEDOT, length 3.5−7.4 nm, with two to six charges per molecule).[61] In fact, the driving forces for oppositely charged polyanion association are known to be "entropic and enthalpic, but not electrostatic".[32] Here, this interplay of molecular forces is observed optically: Many PEDOT molecules are replaced by significantly fewer PDADMA molecules.

With ellipsometry, UV/vis−IR absorbance, and AFM, we investigated PDADMA/PEDOT:PSS multilayers. The observation of PEDOT:PSS nanoparticle monolayers (thickness ≈ 70 nm) was unexpected. The first PEDOT:PSS adsorption layer prepared by dip coating is a nanoparticle monolayer. If the washing step of PEDOT:PSS terminated multilayer prepared by flow cell (0.2 mL/min) is omitted, then a PEDOT:PSS nanoparticle monolayer is found on top of the thin PEDOT:PSS layer. The absorbance of the nanoparticle monolayer varies. The highest value was observed for the monolayer prepared by dip coating (0.163), but it can be drastically reduced by adsorption of PDADMA on top of the monolayer. In this case, PDADMA replaces PEDOT. The absorbance of the nanoparticle monolayer observed in the nonwashed film prepared by flow cell was smaller (0.11) than that of the nanoparticle monolayer prepared by dip coating but still an order of magnitude larger than that of a PEDOT:PSS bilayer (0.015).

These observations lead to a simple model for the formation of the PEDOT:PSS adsorption layers: (1) a PEDOT:PSS nanoparticle monolayer adsorbs, (2) the PSS molecules within the PEDOT:PSS nanoparticle monolayer rearrange: PSS with electrostatically bound PEDOT adsorbs directly to the positively charged substrate and remains there, even (3) when the altered nanoparticle monolayer desorbs. It desorbs when the film is removed from the adsorption solution (dip-coating) or when the washing solution flows over the film (flow cell).

3.5. Electrical Properties. The resistance R of each PDADMA/PEDOT:PSS film was determined using the setup shown in Scheme 3. The thickness d of the films was taken from the ellipsometry measurements (Figure 2); the length L and width W were a few centimeters. For all PDADMA/PEDOT:PSS films, we observed a linear relationship between the applied voltage U and the measured current I, as expected by Ohm's law (Figure S5a,b). In the case of the films prepared by dip coating, the ohmic behavior was maintained up to 12 V, whereas the films prepared by flow cell showed ohmic behavior up to 6 V.

We measured the conductivity parallel and perpendicular to the flow direction for a (PEDOT:PSS/PDADMA)$_2$ film prepared by the flow cell. The DC current was the same, and there was no anisotropy.

Figure 6a shows the sheet resistance R_S of the films calculated with eq 1. It decreases with each additional PDADMA/PEDOT:PSS bilayer. Always, the films prepared by dip coating show a larger R_S than the films prepared by flow cell. For the films prepared by dip coating, R_S can be tuned by up to an order of magnitude (from 10 kΩ for two PDADMA/PEDOT:PSS bilayers to 0.77 kΩ for eight bilayers). Similarly, the sheet resistance of films prepared by flow cell can be tuned by a factor of about six (from 0.3 to 0.05 kΩ). Combining both preparation methods, R_S can be adjusted by more than 2 orders of magnitude.

The (PDADMA/PEDOT:PSS) bilayers have a constant thickness; absorption measurements indicates that they have a constant PEDOT coverage. We therefore assume that they also have a constant electrical conductivity ($\sigma = 1/\rho$). To calculate σ with eq 1, the inverse sheet resistance is shown in dependence of the film thickness (Figure 6b). However, the films prepared by dip coating start with a ≈70 nm thick PEDOT:PSS nanoparticle monolayer. Therefore, eq 1 is modified.

$$\rho = R_S \frac{W \cdot (d - d_0)}{L} \tag{2}$$

d_0 denotes the thickness of a nonconducting base layer. For films prepared by the flow cell, $d_{0,flow} \approx 0$ nm. However, for the films prepared by dip coating, $d_{0,dip} \approx 96$ nm. $d_{0,dip}$ is similar to the thickness of the PEDOT:PSS nanoparticle monolayer (≈70 nm). The nanoparticle monolayer lost its PEDOT during PDADMA adsorption. Without PEDOT, the former PEDOT:PSS nanoparticle monolayer forms the nonelectrically conductive base layer, contributing to the film thickness.

The electrical conductivity $\sigma = 1/\rho$ was deduced from the slope of a linear fit of sheet resistance R_S versus film thickness d. Films prepared by flow cell showed a higher sheet resistance than those prepared by dip coating (230 and 26 kS/m, respectively). The films prepared by flow cell have a

https://doi.org/10.1021/acsomega.4c08946
ACS Omega 2024, 9, 48810−48820

conductivity that exceeds the benchmark value for spin-coated PEDOT:PSS films (100 kS/m).[1−3]

These results show that building multilayer films from PEDOT:PSS with electrical conductivity above 100 kS/m (1000 S/cm) and adjustable film thickness is possible (with EG and GOPS in the PEDOT:PSS dispersion as described for spin-coated films). The high PEDOT coverage observed in the films prepared by dip-coating does not produce high electrical conductivity. In contrast, the films prepared by flow cell and a factor of 3 lower PEDOT coverage per deposited bilayer (according to absorbance) showed an order of magnitude higher electrical conductivity. While polarons and bipolarons are very mobile within a PEDOT molecule, the electrical conductivity of a film is achieved by charge carrier transport between the PEDOT molecules.

The low film/air roughness observed with the AFM suggests the reason for the high electrical conductivity: during PEDOT:PSS adsorption, the PSS chains with associated PEDOT in PEDOT:PSS nanoparticles not only rearrange and partly desorb, the PEDOT molecules adsorb in an approximately flat orientation. We propose that a network of nearly flat, associated PEDOT molecules is necessary to enable large charge carrier mobility and high electrical conductivity.

4. CONCLUSIONS

In the context of creating thin electrically conductive layers for biological applications, a series of multilayers were prepared by sequential adsorption of polycation PDAMA (from a 0.1 M NaCl solution) and negatively charged PEDOT:PSS from a PEDOT:PSS nanoparticle dispersion. PEDOT is in the center of the PEDOT:PSS nanoparticles.

This system is interesting because the electrostatic bonds between PSS and PEDOT are weak. Every third to fifth PEDOT repeat unit is positively charged and can bind electrostatically to the strong polyelectrolyte PSS. The adsorption conditions influence the orientation and coverage of PEDOT.

We find and describe PEDOT:PSS nanoparticle monolayers: The first PEDOT:PSS adsorption layer prepared by dip coating is such a nanoparticle monolayer (thickness ≈ 70 nm, PEDOT absorbance 0.16). The top PEDOT:PSS layer of a PDADMA/PEDOT:PSS multilayer prepared by flow cell (0.2 mL/min) is thin (thickness of a PDADMA/PEDOT:PSS bilayer 7.5 nm).- Unexpectedly, if the last washing step is omitted, then a PEDOT:PSS nanoparticle monolayer is found on top of the thin PEDOT:PSS layer. It has the same thickness as observed before but a smaller absorbance (≈70 nm, PEDOT absorbance 0.11).

These observations lead to a model for the formation of a PEDOT:PSS adsorption layer based on several steps: (1) a PEDOT:PSS nanoparticle monolayer adsorbs, (2) the PSS molecules within the PEDOT:PSS nanoparticle monolayer rearrange: PSS with electrostatically bound PEDOT adsorbs directly to the positively charged substrate and remains there, while (3) the altered nanoparticle monolayer desorbs. How the nanoparticle monolayer desorbs depends on the preparation method: either when the film is removed from the adsorption solution (films prepared by dip-coating) or when a washing solution flows over the multilayer film in the flow cell.

Films prepared by flow cell (rate 0.2 mL/min) or by dip coating showed a constant thickness per PDADMA/PEDOT:PSS bilayer (flow cell 7.5 nm and dip coating 9.5 nm) when the film consisted of at least two PDADMA/PEDOT:PSS bilayers. The electrical conductivity was constant for each preparation method and independent of the number of deposited bilayers.

The electrical conductivity was of the PDADMA/PEDOT:PSS films prepared by flow cell was an order of magnitude higher (230 kS/m-) than that of the films prepared by dip coating (26 kS/m). It exceeded the electrical conductivity of spin-coated films (100 kS/m). This was unexpected since the PEDOT coverage per deposited PEDOT:PSS/PDADMA bilayer is a factor of 3 higher for films prepared by dip coating. However, the improved electrical conductivity correlates with the reduced roughness of the film/air interface. It highlights the importance of the orientation of the PEDOT molecules relative to the substrate for charge carrier mobility. The reduced roughness is only achieved in the flow cell when a flow rate above a certain threshold is used.

These are the first experiments; a better understanding and control of PEDOT:PSS adsorption may further increase the conductivity of multilayer films made from PEDOT:PSS.

■ ASSOCIATED CONTENT

Supporting Information

The Supporting Information is available free of charge at https://pubs.acs.org/doi/10.1021/acsomega.4c08946.

Photographs of the home-built flow cell (Figure S1). Absorbance deduced from PEDOT spectra (430, 500, and 700 nm, Figure S2) and the maximum of the PSS absorption peak (225 nm, Figure S3) at different wavelengths for (PEI/PSS)/(PDADMA/PEDOT:PSS)2 films prepared in the flow cell at different flow rates. UV/vis−NIR absorbance spectra (Figure S4) and $U-I$ diagrams (Figure S5) of PEI/PSS/(PDADMA/PEDOT:PSS)$_N$ multilayers; the films were prepared by dip coating and flow cell. Parameters of the different slabs used for mean square fits of ellipsometry data (Table S1) (PDF)

■ AUTHOR INFORMATION

Corresponding Author

Christiane A. Helm − *Institute of Physics, University of Greifswald, D-17489 Greifswald, Germany;* orcid.org/0000-0001-5181-1688; Email: helm@physik.uni-greifswald.de

Authors

Muhammad Khurram − *Institute of Physics, University of Greifswald, D-17489 Greifswald, Germany*

Sven Neuber − *Institute of Physics, University of Greifswald, D-17489 Greifswald, Germany*

Annekatrin Sill − *Institute of Physics, University of Greifswald, D-17489 Greifswald, Germany;* orcid.org/0000-0002-5454-1289

Complete contact information is available at: https://pubs.acs.org/10.1021/acsomega.4c08946

Notes

The authors declare no competing financial interest.

■ ACKNOWLEDGMENTS

We are grateful for the financial support of the Deutsche Forschungsgemeinschaft (DFG, German Research Founda-

tion) Collaborative Research Centre (CRC) ELAINE (SFB 1270/2-299150580). We also thank Mr. Frank Scheffter for his technical support and the manufacture of flow cells and Dr. Heiko Ahrens for programming the flow cell.

REFERENCES

(1) Hill, I. M.; Hernandez, V.; Xu, B.; Piceno, J. A.; Misiaszek, J.; Giglio, A.; Junez, E.; Chen, J.; Ashby, P. D.; Jordan, R. S.; Wang, Y. Imparting high conductivity to 3D printed PEDOT:PSS. *ACS Appl. Polym. Mater.* **2023**, *5* (6), 3989−3998.
(2) Ouyang, J. "Secondary doping" methods to significantly enhance the conductivity of PEDOT:PSS for its application as transparent electrode of optoelectronic devices. *Displays* **2013**, *34* (5), 423−436.
(3) Shi, H.; Liu, C.; Jiang, Q.; Xu, J. Effective approaches to improve the electrical conductivity of PEDOT:PSS: A review. *Adv. Electron. Mater.* **2015**, *1* (4), No. 1500017.
(4) Zhang, G.; Chen, Z.; Ahn, C. H.; Suo, Z. Conducting polymer coatings prepared by mixed emulsions are highly conductive and stable in water. *Adv. Mater.* **2024**, *36* (13), No. 2306960.
(5) Håkansson, A.; Han, S.; Wang, S.; Lu, J.; Braun, S.; Fahlman, M.; Berggren, M.; Crispin, X.; Fabiano, S. Effect of (3-glycidyloxypropyl) trimethoxysilane (GOPS) on the electrical properties of PEDOT:PSS films. *J. Polym. Sci., Part B: Polym. Phys.* **2017**, *55* (10), 814−820.
(6) Wen, Y.; Xu, J. Scientific importance of water-processable PEDOT−PSS and preparation, challenge and new application in sensors of its film electrode: A review. *J. Polym. Sci., Part A: Polym. Chem.* **2017**, *55* (7), 1121−1150.
(7) Kim, S.-M.; Kim, C.-H.; Kim, Y.; Kim, N.; Lee, W.-J.; Lee, E.-H.; Kim, D.; Park, S.; Lee, K.; Rivnay, J.; Yoon, M. H. Influence of PEDOT:PSS crystallinity and composition on electrochemical transistor performance and long-term stability. *Nat. Commun.* **2018**, *9* (1), No. 3858.
(8) Decher, G.; Hong, J. D.; Schmitt, J. Buildup of ultrathin multilayer films by a self-assembly process: III. Consecutively alternating adsorption of anionic and cationic polyelectrolytes on charged surfaces. *Thin Solid Films* **1992**, *210−211*, 831−835.
(9) Boudou, T.; Crouzier, T.; Ren, K.; Blin, G.; Picart, C. Multiple functionalities of polyelectrolyte multilayer films: New biomedical applications. *Adv. Mater.* **2010**, *22* (4), 441−467.
(10) Neuber, S.; Sill, A.; Efthimiopoulos, I.; Nestler, P.; Fricke, K.; Helm, C. A. Influence of molecular weight of polycation polydimethyldiallylammonium and carbon nanotube content on electric conductivity of layer-by-layer films. *Thin Solid Films* **2022**, *745*, No. 139103.
(11) Neuber, S.; Sill, A.; Ahrens, H.; Quade, A.; Helm, C. A. Influence of different solutions on electrically conductive films composed of carbon nanotubes and polydimethyldiallylammonium. *ACS Appl. Eng. Mater.* **2023**, *1* (6), 1493−1503.
(12) Durstock, M. F.; Rubner, M. F. Dielectric properties of polyelectrolyte multilayers. *Langmuir* **2001**, *17* (25), 7865−7872.
(13) DeLongchamp, D. M.; Hammond, P. T. Fast ion conduction in layer-by-layer polymer films. *Chem. Mater.* **2003**, *15* (5), 1165−1173.
(14) DeLongchamp, D. M.; Hammond, P. T. Highly ion conductive poly (ethylene oxide)-based solid polymer electrolytes from hydrogen bonding layer-by-layer assembly. *Langmuir* **2004**, *20* (13), 5403−5411.
(15) Nicolas, H.; Yuan, B.; Xu, J.; Zhang, X.; Schönhoff, M. pH-responsive host−guest complexation in pillar [6] arene-containing polyelectrolyte multilayer films. *Polymers* **2017**, *9* (12), 719.
(16) Li, W.; Liu, J.; Tang, K.; Mao, X.; Jin, S.; Deng, R.; Zhu, J. Functional materials of 2D self-assembled nanoparticle monolayers: Preparation and application. *Chem. Mater.* **2024**, *36* (19), 9279−9298.
(17) Ostendorf, A.; Cramer, C.; Decher, G.; Schönhoff, M. Humidity-tunable electronic conductivity of polyelectrolyte multilayers containing gold nanoparticles. *J. Phys. Chem. C* **2015**, *119* (17), 9543−9549.
(18) Echols, I. J.; An, H.; Yun, J.; Sarang, K. T.; Oh, J.-H.; Habib, T.; Zhao, X.; Cao, H.; Holta, D. E.; Radovic, M.; et al. Electronic and optical property control of polycation/MXene layer-by-layer assemblies with chemically diverse MXenes. *Langmuir* **2021**, *37* (38), 11338−11350.
(19) Groenendaal, L.; Jonas, F.; Freitag, D.; Pielartzik, H.; Reynolds, J. R. Poly(3, 4-ethylenedioxythiophene) and its derivatives: Past, present, and future. *Adv. Mater.* **2000**, *12* (7), 481−494.
(20) Dimitriev, O. P.; Piryatinski, Y. P.; Pud, A. A. Evidence of the controlled interaction between PEDOT and PSS in the PEDOT:PSS complex via concentration changes of the complex solution. *J. Phys. Chem. B* **2011**, *115* (6), 1357−1362.
(21) Li, Y.; Tanigawa, R.; Okuzaki, H. Soft and flexible PEDOT/PSS films for applications to soft actuators. *Smart Mater. Struct.* **2014**, *23* (7), No. 074010.
(22) Hosseini, E.; Kollath, V. O.; Karan, K. The key mechanism of conductivity in PEDOT:PSS thin films exposed by anomalous conduction behaviour upon solvent-doping and sulfuric acid post-treatment. *J. Mater. Chem. C* **2020**, *8* (12), 3982−3990.
(23) Rivnay, J.; Inal, S.; Collins, B. A.; Sessolo, M.; Stavrinidou, E.; Strakosas, X.; Tassone, C.; Delongchamp, D. M.; Malliaras, G. G. Structural control of mixed ionic and electronic transport in conducting polymers. *Nat. Commun.* **2016**, *7* (1), No. 11287.
(24) Lu, B.; Yuk, H.; Lin, S.; Jian, N.; Qu, K.; Xu, J.; Zhao, X. Pure PEDOT:PSS hydrogels. *Nat. Commun.* **2019**, *10* (1), No. 1043.
(25) Oechsle, A. L.; Heger, J. E.; Li, N.; Yin, S.; Bernstorff, S.; Müller-Buschbaum, P. Correlation of thermoelectric performance, domain morphology and doping level in PEDOT:PSS thin films post-treated with ionic liquids. *Macromol. Rapid Commun.* **2021**, *42* (20), No. 2100397.
(26) Nardes, A. M.; Kemerink, M.; Janssen, R. A.; Bastiaansen, J. A.; Kiggen, N. M.; Langeveld, B. M.; Van Breemen, A. J.; De Kok, M. M. Microscopic understanding of the anisotropic conductivity of PEDOT:PSS thin films. *Adv. Mater.* **2007**, *19* (9), 1196−1200.
(27) Kim, N.; Lee, B. H.; Choi, D.; Kim, G.; Kim, H.; Kim, J.-R.; Lee, J.; Kahng, Y. H.; Lee, K. Role of interchain coupling in the metallic state of conducting polymers. *Phys. Rev. Lett.* **2012**, *109* (10), No. 106405.
(28) Palumbiny, C. M.; Liu, F.; Russell, T. P.; Hexemer, A.; Wang, C.; Müller-Buschbaum, P. The crystallization of PEDOT:PSS polymeric electrodes probed in situ during printing. *Adv. Mater.* **2015**, *27* (27), 3391−3397.
(29) Kroon, R.; Mengistie, D. A.; Kiefer, D.; Hynynen, J.; Ryan, J. D.; Yu, L.; Müller, C. Thermoelectric plastics: From design to synthesis, processing and structure−property relationships. *Chem. Soc. Rev.* **2016**, *45* (22), 6147−6164.
(30) Franco-Gonzalez, J. F.; Zozoulenko, I. V. Molecular dynamics study of morphology of doped PEDOT: From solution to dry phase. *J. Phys. Chem. B* **2017**, *121* (16), 4299−4307.
(31) Gutierrez-Fernandez, E.; Ezquerra, T. A.; García-Gutiérrez, M.-C. Additive effect on the structure of PEDOT:PSS dispersions and its correlation with the structure and morphology of thin films. *Polymers* **2022**, *14* (1), 141.
(32) Aasmundtveit, K.; Samuelsen, E.; Pettersson, L.; Inganäs, O.; Johansson, T.; Feidenhans, R. Structure of thin films of poly (3, 4-ethylenedioxythiophene). *Synth. Met.* **1999**, *101* (1−3), 561−564.
(33) Sill, A.; Nestler, P.; Azinfar, A.; Helm, C. A. Tailorable polyanion diffusion coefficient in LbL films: The role of polycation molecular weight and polymer conformation. *Macromolecules* **2019**, *52* (22), 9045−9052.
(34) Richardson, J. J.; Björnmalm, M.; Caruso, F. Technology-driven layer-by-layer assembly of nanofilms. *Science* **2015**, *348* (6233), No. aaa2491.
(35) de Saint-Aubin, C.; Hemmerlé, J.; Boulmedais, F.; Vallat, M.-F.; Nardin, M.; Schaaf, P. New 2-in-1 polyelectrolyte step-by-step film buildup without solution alternation: From PEDOT-PSS to polyelectrolyte complexes. *Langmuir* **2012**, *28* (23), 8681−8691.
(36) DeLongchamp, D.; Hammond, P. T. Layer-by-layer assembly of PEDOT/polyaniline electrochromic devices. *Adv. Mater.* **2001**, *13* (19), 1455−1459.

https://doi.org/10.1021/acsomega.4c08946
ACS Omega 2024, 9, 48810−48820

(37) Anand, A.; Madalaimuthu, J. P.; Schaal, M.; Otto, F.; Gruenewald, M.; Alam, S.; Fritz, T.; Schubert, U. S.; Hoppe, H. Why organic electronic devices comprising PEDOT:PSS electrodes should be fabricated on metal free substrates. *ACS Appl. Electron. Mater.* **2021**, *3* (2), 929−943.
(38) Wei, T.-C.; Chen, S.-H.; Chen, C.-Y. Highly conductive PEDOT:PSS film made with ethylene-glycol addition and heated-stir treatment for enhanced photovoltaic performances. *Mater. Chem. Front.* **2020**, *4* (11), 3302−3309.
(39) Lin, Y.-J.; Ni, W.-S.; Lee, J.-Y. Effect of incorporation of ethylene glycol into PEDOT:PSS on electron phonon coupling and conductivity. *J. Appl. Phys.* **2015**, *117* (21), 215501.
(40) Kergoat, L.; Piro, B.; Simon, D. T.; Pham, M. C.; Noël, V.; Berggren, M. Detection of glutamate and acetylcholine with organic electrochemical transistors based on conducting polymer/platinum nanoparticle composites. *Adv. Mater.* **2014**, *26* (32), 5658−5664.
(41) Berezhetska, O.; Liberelle, B.; De Crescenzo, G.; Cicoira, F. A simple approach for protein covalent grafting on conducting polymer films. *J. Mater. Chem. B* **2015**, *3* (25), 5087−5094.
(42) Kern, W. The evolution of silicon wafer cleaning technology. *J. Electrochem. Soc.* **1990**, *137* (6), 1887.
(43) Lipton, J.; Weng, G.-M.; Röhr, J. A.; Wang, H.; Taylor, A. D. Layer-by-layer assembly of two-dimensional materials: Meticulous control on the nanoscale. *Matter* **2020**, *2* (5), 1148−1165.
(44) Nicolas, H.; Yuan, B.; Zhang, J.; Zhang, X.; Schönhoff, M. Cucurbit [8] uril as nanocontainer in a polyelectrolyte multilayer film: A quantitative and kinetic study of guest uptake. *Langmuir* **2015**, *31* (39), 10734−10742.
(45) Gresham, I. J.; Reurink, D. M.; Prescott, S. W.; Nelson, A. R.; De Vos, W. M.; Willott, J. D. Structure and hydration of asymmetric polyelectrolyte multilayers as studied by neutron reflectometry: Connecting multilayer structure to superior membrane performance. *Macromolecules* **2020**, *53* (23), 10644−10654.
(46) Sill, A.; Nestler, P.; Weltmeyer, A.; Paßvogel, M.; Neuber, S.; Helm, C. A. Polyelectrolyte multilayer films from mixtures of polyanions: Different compositions in films and deposition solutions. *Macromolecules* **2020**, *53* (16), 7107−7118.
(47) Nestler, P.; Paßvogel, M.; Ahrens, H.; Soltwedel, O.; Köhler, R.; Helm, C. A. Branched poly (ethylenimine) as barrier layer for polyelectrolyte diffusion in multilayer films. *Macromolecules* **2015**, *48* (23), 8546−8556.
(48) Sill, A.; Nestler, P.; Thran, P.; Helm, C. A. Dependence of PSS diffusion in multilayers of entangled PDADMA on temperature and salt concentration: More than one diffusion constant. *Macromolecules* **2021**, *54* (20), 9372−9384.
(49) Löhmann, O.; Micciulla, S.; Soltwedel, O.; Schneck, E.; von Klitzing, R. Swelling behavior of composite systems: Mutual effects between polyelectrolyte brushes and multilayers. *Macromolecules* **2018**, *51* (8), 2996−3005.
(50) Nestler, P.; Block, S.; Helm, C. A. Temperature-induced transition from odd−even to even−odd effect in polyelectrolyte multilayers due to interpolyelectrolyte interactions. *J. Phys. Chem. B* **2012**, *116* (4), 1234−1243.
(51) Nestler, P.; Helm, C. A. Determination of refractive index and layer thickness of nm-thin films via ellipsometry. *Opt. Express* **2017**, *25* (22), 27077−27085.
(52) Azzam, R. M. A.; Bashara, N. M.; Ballard, S. S. Ellipsometry and polarized light. *Phys. Today* **1978**, *31* (11), 72.
(53) Runde, S.; Ahrens, H.; Lawrenz, F.; Sebastian, A.; Block, S.; Helm, C. A. Stable 2D conductive Ga/Ga (OxHy) multilayers with controlled nanoscale thickness prepared from gallium droplets with oxide skin. *Adv. Mater. Interfaces* **2018**, *5* (16), No. 1800323.
(54) Webster, J. G. *Electrical Measurement, Signal Processing, and Displays*; CRC Press, 2003.
(55) Büscher, K.; Graf, K.; Ahrens, H.; Helm, C. A. Influence of adsorption conditions on the structure of polyelectrolyte multilayers. *Langmuir* **2002**, *18* (9), 3585−3591.
(56) Choi, J.; Rubner, M. F. Influence of the degree of ionization on weak polyelectrolyte multilayer assembly. *Macromolecules* **2005**, *38* (1), 116−124.
(57) McAloney, R. A.; Sinyor, M.; Dudnik, V.; Goh, M. C. Atomic force microscopy studies of salt effects on polyelectrolyte multilayer film morphology. *Langmuir* **2001**, *17* (21), 6655−6663.
(58) Guzmán, E.; Ritacco, H.; Rubio, J. E.; Rubio, R. G.; Ortega, F. Salt-induced changes in the growth of polyelectrolyte layers of poly (diallyl-dimethylammonium chloride) and poly (4-styrene sulfonate of sodium). *Soft Matter* **2009**, *5* (10), 2130−2142.
(59) Dauzon, E.; Mansour, A. E.; Niazi, M. R.; Munir, R.; Smilgies, D.-M.; Sallenave, X.; Plesse, C.; Goubard, F.; Amassian, A. Conducting and stretchable PEDOT:PSS electrodes: Role of additives on self-assembly, morphology, and transport. *ACS Appl. Mater. Interfaces* **2019**, *11* (19), 17570−17582.
(60) Saha, A.; Ohori, D.; Sasaki, T.; Itoh, K.; Oshima, R.; Samukawa, S. Effect of film morphology on electrical conductivity of PEDOT:PSS. *Nanomaterials* **2024**, *14* (1), 95.
(61) Fu, J.; Schlenoff, J. B. Driving forces for oppositely charged polyion association in aqueous solutions: Enthalpic, entropic, but not electrostatic. *J. Am. Chem. Soc.* **2016**, *138* (3), 980−990.

https://doi.org/10.1021/acsomega.4c08946
ACS Omega 2024, 9, 48810−48820